

**Tethering of Mitral Leaflets Relates to Displacement of Papillary Muscles
by Dislocation of Heart during Off-pump Coronary Artery Bypass Surgery:
Assessment of Deformation of Mitral Valve Complex using
Three-dimensional Echocardiography in Porcine Model**

心拍動下冠動脈バイパス術における僧帽弁尖のテザリングは

心脱転に伴う乳頭筋変位と関連する：

ブタモデルにおける 3 次元心エコー図法による

僧帽弁装置の形態学的変化の評価

Igarashi Takashi,

Cardiovascular Surgery, Fukushima Medical University

福島県立医科大学 心臓血管外科学講座

五十嵐崇

Abstract

BACKGROUND: Intraoperative worsening of mitral regurgitation is one of the causes of the hemodynamic deterioration during off-pump coronary artery bypass grafting (OPCAB) in ischemic heart disease. However, the deformation of the mitral valve complex during the dislocation of the beating heart during OPCAB remains unclear.

OBJECTIVES: To clarify the mechanism of the mitral regurgitation during OPCAB, we assessed the deformation of mitral valve complex in the dislocation of the beating heart using by three-dimensional echocardiography.

METHODS: In 9 healthy swine with median sternotomy, we positioned the beating heart as OPCAB model i.e., control, left anterior descending artery (LAD), right coronary artery (RCA) and left circumflex artery (LCX) positions. In 4 positions, three-dimensional echocardiography was performed to assess mitral valve complex with hemodynamic parameters. We analyzed the deformation of mitral valve and three-dimensional coordinate of papillary muscles in each position.

RESULTS: The systolic and diastolic blood pressures were decreased in LCX position compared to control (control vs LCX: 69.8 ± 2.7 vs 48.9 ± 2.5 mmHg, $P < 0.001$). There were no significant differences in the mitral annular diameters in each position. However, there were significantly increased in the maximum tenting length (control 2.9 ± 1.3 , LAD 2.7 ± 1.0 , RCA 3.7 ± 0.9 , LCX 4.1 ± 0.9 mm, $P < 0.01$), the mean tenting length (control 0.65 ± 1.01 , LAD 0.46 ± 0.84 , RCA 1.31 ± 0.60 , LCX 1.54 ± 0.63 mm, $P < 0.01$) and the tenting volume (control

0.70±0.30, LAD 0.65±0.27, RCA 0.79±0.23, LCX 0.95±0.34 cm³, $P < 0.05$) in LCX than the other positions. The angle α (between the posterior papillary muscle-to-annulus line and the annular plane) has significantly relationship with the tenting volume ($r = -0.643$, $P < 0.001$). The posterior papillary muscle was displaced to medial side in LAD and LCX position ($P < 0.01$).

CONCLUSION: Our study suggests that dislocation of beating heart during OPCAB cause displacement of papillary muscle associated with the geometric change of left ventricle, resulting in mitral valve tethering with exacerbation of both mitral regurgitation and hemodynamics .

Key Words

OPCAB, mitral valve complex, mitral regurgitation, tethering, three-dimensional echocardiography

Introduction

Avoiding extracorporeal circulation, manipulation of the aorta and cardiac arrest, off-pump coronary artery bypass grafting (OPCAB) is a safe, minimally invasive surgery for high-risk patients [1-4], especially with advanced age, low ejection fraction, chronic obstructive pulmonary disease, renal insufficiency, and atheromatous disease of the ascending aorta. Recently, OPCAB disseminated widely around the world, accounting about 65% of all coronary artery bypass grafting (CABG) in Japan, 15-20% in United States of America and European Union.

During OPCAB, it is important to stabilize the hemodynamics especially when surgeon needs elevation and dislocation of the beating heart [5-9]. Several clinical investigations reported that the operative mortality is higher in cases with hemodynamic instability with consequent urgent pump conversion during OPCAB, rather than in cases with conventional on-pump arrested CABG [6,7,9]. Although several predictors for the hemodynamic instability during OPCAB have been reported [5,6,8,10], intraoperative worsening of the mitral regurgitation (MR) is one of the significant predictors [5,10-12], that is often observed during elevation and dislocation of the beating heart.

A few recent investigations have reported deformation of mitral valve complex related to MR during OPCAB. Koga and colleagues reported that the displacement of the beating heart combined with the occlusion of the left circumflex artery (LCX) caused mitral regurgitation from the posteromedial site of the mitral valve due to the enlargement of posteromedial dimension of the mitral annulus in an OPCAB animal model [13]. George and colleagues reported

that mitral valve was folded and twisted in the dislocated position in the patients during OPCAB [12]. However, the mechanism of the worsening of the MR during the dislocation of the beating heart in OPCAB still remains unclear.

In this study, we hypothesized that the deformation of the mitral valve complex such as leaflet, annulus, chorda and papillary muscle, cause the worsening of the MR. The aim of this study is to reveal the mechanism of the worsening of the MR during the dislocation of the heart in OPCAB surgery by the analysis of the deformation of the mitral valve complex using three-dimensional echocardiography.

METHODS

Animal preparation

Female Landrace large white Duroc pigs (n = 9; Saitama Experimental Animals Supply Co., Ltd, Saitama, Japan) weighting 50.5 ± 2.5 kg on cholesterol- free diet were used humanely in compliance with the “Principles of Laboratory Animal Care” formulated by the National Society for Medical Research and the “Guide for the Care and Use of Laboratory Animals” prepared by the Institute of Laboratory Animals Resources and published by the National Institutes of Health (Publication No. 86-23, revised 1985). This study was approved by the institutional ethics committee of Fukushima Medical University [Figure 1].

After anesthesia with an intramuscular injection of ketamine (20 mg/kg, Ketalar[®]; Daiichi Sankyo Propharma Co., Ltd, Tokyo, Japan), atropine (1 mg, Atropine Sulfate[®]; Mylan Co., Tokyo, Japan), and pentobarbital sodium (30

mg/kg, Somnopentyl[®]; Kyoritsu Seiyaku Co., Tokyo, Japan) into the neck, the pig was placed on an operating table in the supine position. An ear vein was cannulated for fluid and drug administration. After tracheotomy and endotracheal intubation, mechanical positive pressure ventilation was maintained with a mixture of 100% oxygen and isoflurane (Forane[®]; Abbvie, Tokyo, Japan) at a tidal volume of 10 mL/kg. Anesthesia was maintained by isoflurane inhalation (0.5%-5%) and a bolus injection of pentobarbital (25 mg/kg).

The external electrocardiogram (lead II) and blood pressure in the femoral artery were continuously monitored. A Swan-Ganz catheter (Baxter Healthcare, Irvine, CA) was inserted from the femoral vein into the pulmonary artery, and the pulmonary artery pressure and the cardiac output were continuously monitored (Vigilance II Monitor[®], Edwards Lifesciences, Irvine, CA, USA). The pericardium was opened through a median sternotomy. To maintain the good heart exposure, the sternal retractor was used. The width of the retractor was 8 cm.

As same as clinical OPCAB surgery, the heart was positioned in 4 positions: control, left anterior descending artery (LAD), right coronary artery (RCA) and left circumflex artery (LCX) positions. In the LAD position, gauze was inserted into the left-side pericardium to displace the apex to the 2 cm right side. In the RCA position, the apex was displaced 1 cm ventral and 3 cm superior in the sagittal plane from the control position with apex suction device (Starfish[™]; Medtronic, Inc., Minneapolis, MN, USA) for the elevation of the apex [14]. In the LCX position, the apex was displaced 4 cm to the right side in the transverse

plane from the RCA position [Figure 2]. In each position, each target coronary artery was mechanically stabilized using a mechanical tissue stabilizer (Octopus 4.3™; Medtronic, Inc., Minneapolis, MN, USA).

Study protocol

In each swine, we positioned the beating heart in 4 different experimental conditions as OPCAB model, i.e., from baseline as control to LAD, RCA, and LCX positions in order.

At first, the hemodynamic and the echocardiographic data were collected in control position. In the next, after the beating heart was set in LAD position for 3 minutes, the hemodynamic and the echocardiographic data were acquired. After the heart was released from the LAD position to control position, we observed the recovery of hemodynamics as same as control. Then, the same procedures were done in the next position (RCA and LCX positions, in order) [Figure 3].

Hemodynamics

In each heart position, we evaluated of the hemodynamic parameters such as heart rate (bpm), cardiac output (L/min) by thermodilution method, systolic, diastolic and mean arterial pressures (mmHg), systolic, diastolic and mean pulmonary artery pressures (mmHg), central venous pressure (mmHg) by fluid-filled method.

Echocardiography

In each position, three-dimensional echocardiographic data were acquired

using iE33[®] (Phillips Healthcare, Andover, USA) with X5-1[®](Frequency: 1-5 MHz), with special attention to visualize mitral valve complex with the tips of papillary muscles from direct approach to the surface of the heart in open chest. The image was recorded by full volume mode in 4 wedge-shaped sub-volumes for 4 consecutive cardiac cycles, and volumetric rate were 28-30 /s.

We evaluated the echocardiographic data in mid-systole for assessment of the change of mitral valve complex in this study.

Assessment of morphology of mitral valve

The three-dimensional morphology of the mitral valve leaflets and annulus was assessed by REALVIEW[®] software (YD Co., Japan) [15,16]. We evaluated the indices of the mitral valve, such as anterior-posterior annular diameter (AP diameter), medial-lateral annular diameter (ML diameter), annular circumference, annular area, annular height, maximum tenting length, mean tenting length and tenting volume [Figure 4].

Evaluation of dislocated papillary muscles

The three-dimensional positions of the tip of papillary muscles were evaluated by Cardioview[®] software (TomTec, Germany) [17] [Figure 5a,b]. We provided each three-dimensional coordinate as follows: A: midpoint of the anterior mitral annulus, B: contralateral point of A on the aortic annulus, C: midpoint of the posterior mitral annulus, APM: the tip of the anterior papillary muscle and PPM: the tip of the posterior papillary muscle [Figure 5a].

We assessed the tethering distances to APM and PPM, and the angle α

defined as between the papillary muscle-to-annulus line and the annular plane (angle α_1 : between APM to A and A to C plane, angle α_2 : between PPM to A and A to C plane) [18][Figure 5b].

Three-dimensional coordinate of papillary muscles

To collect the variation of direction in acquiring of echocardiographic image during each position, three-dimensional coordinates were revised as follows: The x-axis was the vector from A to B. The y-axis was the vector passed the point A and met the x-axis at right angles. The z-axis was the vector passed the point A and met these axes at right angles [Figure 5a]. Thus, it is possible to compare the change of three-dimensional coordinate of papillary muscles in each position, and assess the change of the tip of papillary muscles' coordinate (x, y, z) in each position.

Statistical analysis

Statistical analysis was performed using SPSS ver. 20TM (SPSS, Chicago, USA). Data were expressed as means \pm SD. Hemodynamic variables, mitral valve complex geometric measures were compared among the positions by repeated measures analysis of variance (ANOVA). Significant differences were explored by Bonferroni method, if appropriate. A P value <0.05 was considered statistically significant.

RESULTS

Hemodynamics

Hemodynamic parameters were summarized in Table 1.

There was no difference in heart rate and cardiac output among each position. On the other hand, there were significantly differences in the systolic blood pressure (control position: 69.9 ± 7.7 , LAD position: 57.2 ± 8.2 , RCA position: 54.1 ± 7.4 , LCX position: 48.9 ± 7.1 mmHg, $P < 0.001$ by ANOVA), the diastolic blood pressure (38.1 ± 5.1 , 31.2 ± 5.7 , 32.0 ± 4.1 , 30.7 ± 5.5 mmHg, $P < 0.001$ by ANOVA) and the mean blood pressure (49.8 ± 5.9 , 42.7 ± 8.0 , 40.4 ± 5.1 , 37.8 ± 6.4 mmHg, $P < 0.001$ by ANOVA). The central venous pressure was also significantly increased in dislocated positions, such as RCA and LCX positions, compared with control position (control position: 8.0 ± 0.9 , LAD position: 8.2 ± 1.2 , RCA position: 8.8 ± 1.2 , LCX position: 9.4 ± 1.9 mmHg, $P = 0.001$). However, the systolic, diastolic and mean pulmonary artery pressures were not changed among the 4 positions.

Deformation of mitral valve complex by three-dimensional echocardiography

There was no MR by echocardiography in this study.

The geometric parameters of the mitral valve were showed in Table 2. There were not differences in the AP diameter, the ML diameter, the annular circumference, the annular area and the annular height among each position. However, it was a significantly increased in the indices of tethering of mitral leaflets, i.e., the maximum tenting length (control position: 2.9 ± 1.3 , LAD position: 2.7 ± 1.0 , RCA position: 3.7 ± 0.9 , LCX position: 4.1 ± 0.9 mm, $p < 0.01$ by ANOVA), the mean tenting length (0.65 ± 1.01 , 0.46 ± 0.84 , 1.31 ± 0.60 , 1.54 ± 0.63 mm, $p < 0.01$ by ANOVA), and the tenting volume (0.70 ± 0.30 , 0.65 ± 0.27 , 0.79 ± 0.23 ,

0.95±0.34 cm³, p<0.05 by ANOVA).

Figure 6 shows the example of change in the mitral leaflets depending on each position. It was revealed that the tenting of mitral leaflets was increased in the dislocated positions, especially in LCX position, compared to the control position [Figure 6].

Change of papillary muscles' positions

The parameters of the papillary muscles' positions were shown in Table 2. There were no differences in the tethering distances to APM and PPM. Although it did not differ in the angle α_1 among each position, the angle α_2 tended to decrease in LCX position compared to control position.

Relation between configuration of mitral valve and papillary muscles' positions

We assessed whether indices of the papillary muscles' position related to the indices in configuration of mitral valve (annular diameters and tenting of mitral leaflets). Among these indices, the angle α_2 had a strong correlation with the tenting volume ($r = -0.643$, $p < 0.001$) and the dislocation of PPM related to the increasing tenting of mitral leaflet [Figure 7a]. A scattergram (right side) showed relation between the control position and the LCX position in each case. This graph revealed that tenting volume tended to increase and angle α_2 tended to decrease by the displacement of the heart in many cases [Figure 7b].

Three-dimensional coordinates of papillary muscles

The three-dimensional coordinates of the papillary muscles in each position were showed in Table 3. There was a significant change of the PPM position in the z-axis direction (control position: -2.9 ± 4.8 mm, LAD position: -9.6 ± 3.6 mm, RCA position: -3.9 ± 3.2 mm, LCX position: -9.3 ± 3.6 mm, $p < 0.01$ by ANOVA).

The displacements of the papillary muscles in each heart position were expressed by schema in Figure 8 (short axis view via apex). In particular, the tip of the PPM and the APM dislocated to the medial side in LCX position. There were the changes of geometry in left ventricle and mitral complex in dislocated beating heart as OPCAB model.

DISCUSSION

The main findings of this study were as follows; 1) The hemodynamics was impaired in association with the dislocation of the beating heart. 2) The tenting of mitral valve leaflets was increased in the dislocated position, especially in LCX position. 3) There was a significant negative correlation between the angle α_2 and the tenting volume. 4) The posterior papillary muscle (PPM) was significantly displaced to medial side in LCX position.

This study revealed that the mitral leaflet tenting was increased associated with the dislocation of PPM, which lead to the change of the towing direction of the mitral leaflet. In LCX position, the PPM was dislocated to the medial side from the relative control position of the mitral valve. The smaller the angle α_2 was, the larger tenting volume was.

In this experimental study, there was no mitral regurgitation. However, it was demonstrated that the leaflet tenting had significant differences in each position

and is an important factor of worsening of the mitral regurgitation. In clinical OPCAB or ischemic animal models, it is adequately considered that displacement of the papillary muscle causes worsening of mitral regurgitation.

The displacement of the PPM may be associated with the surgical technique for dislocation of the beating heart. The dislocation of the beating heart was achieved by using the apical suction device. In LCX position, the apex was elevated to the ventral and the superior direction in the sagittal plane and the right side in the transverse plane. Probably because the geometry of the left ventricle was changes by the pliability and the extensibility of the left ventricle, the relative positions among the inner structures of the left ventricle including the mitral complex were not preserved. The geometry of apex and the mitral valve was also changed significantly by the traction of the apex in OPCAB. The PPM can be moved to the medial site by the traction of the apex. These changes occurred in the relative position among the PPM, the mitral leaflets and the posterior wall of the LV.

Thus, the position of PPM seems to play a major role in the cause of tethered mitral valve leaflets in OPCAB. This finding has a close similarity with the worsening of ischemic mitral regurgitation in the inferior-posterior myocardial infarction. Mitral regurgitation in ischemic heart disease has been investigated recently. Some investigators reported that the papillary muscles displacement caused by the LV dilatation result in the increasing of the tenting of the mitral leaflets and the tethering distance in patients with ischemic mitral regurgitation [19-21]. Kumanohoso and colleagues reported the echocardiographic analysis in patients with prior anterior and inferior myocardial infarction [19]. They

demonstrated that the posterior papillary muscle-tethering distance was significantly greater in patients with myocardial infarction in inferior wall compared in anterior wall, and an independent contributing factor in the grade of mitral regurgitation was the increasing in posterior papillary muscle-tethering distance [19]. In such ischemic patients, there is already a certain degree of tethering or poor coaptation of mitral leaflets. Therefore, there may a similarity in the exacerbation of severe mitral regurgitation caused by increasing of the tethering due to the dislocation of the heart in OPCAB.

This study showed no difference in the tethering distance of the both papillary muscles, suggesting that the increase of the leaflet tenting can occur even if there is only the change of the towing direction of the mitral leaflet without the increase of the tethering distance during beating heart surgery. However, because the present study was an acute animal experimental study in non-ischemic models, the tethering distances might not be changed. In addition, there was no progression of mitral regurgitation caused by the dislocation of the heart in this study. Because the coaptation of the mitral leaflets was well reserved adequately in healthy swine, the worsening of the tethering in the dislocated position may not lead to the MR worsening in this specific experimental settings.

This study showed no significant change of the mitral annulus by the dislocation of the beating heart. Koga and associates reported that the displacement of the beating heart in addition to occlusion of the left circumflex artery (LCX) caused mitral regurgitation from the posteromedial site of the mitral valve, with enlarged posteromedial dimension of the annulus in OPCAB dog models [13]. This difference may depend on the experimental model with or

without ischemia.

It was thought the low arterial pressure in control position was affected the anesthesia. In dislocated position, especially in LCX position, we think that the cause of hypotension is multifactorial, and the restriction on systolic and diastolic LV motion caused by the dislocation of the heart was the most important factor affected the hypotension. Ozay et al reported that, in their clinical study, the ejection fraction decreased significantly during LCX and RCA position, and the wall motion score index was significantly increased during LCX position compared other positions. They also described that these findings returned to baseline at the end of the operation [5]. This result indicates a reversible regional systolic dysfunction during LCX position. Akazawa et al also reported that factors causing deterioration in hemodynamics during OPCAB include myocardial ischemia, cardiac chamber compression, reduced ventricular filling and reduced diastolic function [10]. Practically, it is thought that newly emerging mitral regurgitation and other factors affected intraoperative hemodynamic instability jointly.

Clinical Implication

First, focusing on the mechanism of the displacement of the PPM during the dislocation of the heart, when mitral regurgitation is worsening in OPCAB, it may be possible to correct the position of the PPM from the surface of inferior wall of LV with trans-esophageal echocardiography guiding.

Second, it may be possible to establish the method of displacement of the heart that hardly causes the dislocation of PPM and worsening MR by analyzing

the relation between the dislocation of the PPM and both the degree and direction of the traction of the apex.

Study Limitations

First, this study was the acute experimental study using healthy, non-ischemic porcine model. Porcine heart is similar to human heart anatomically, however, there was small difference of the attached part of the papillary muscles between in swine and in human. It seems also mandatory to analyze the heart with ischemia and/or infarction.

Second, we assessed the morphology of mitral complex in only mid-systole. It remains unclear whether the dislocation of the heart affects the motion of mitral complex in each phase of the cardiac cycle.

Conclusions

This study suggested that the deformation in the mitral valve complex during the dislocation of the beating heart play an important role in the worsening of mitral regurgitation and the hemodynamic instability in OPCAB. The prime cause of the increase of tenting of mitral leaflets is suggested the displacement of the posterior papillary muscle associated with the change in geometry of the left ventricle.

References

1. Marek Polonsky, John D. Puskas. Off-pump coronary artery bypass grafting--the current state. *Circ J* 2012;76(4):784-90.
2. John D. Puskas, Vinod H. Thourani, Patrick Kilgo, et al. Off-pump coronary artery bypass disproportionately benefits high-risk patients. *Ann Thorac Surg* 2009;88(4):1142-7.
3. Eric L. Sarin, Michael O. Kayatta, Patrick Kilgo, et al. Short- and long-term outcomes in octogenarian patients undergoing off-pump coronary artery bypass grafting compared with on-pump coronary artery bypass grafting. *Innovations* 2011;6(2):110-5.
4. W. Brent Keeling, Matthew L. Williams, Mark S. Slaughter, et al. Off-pump and on-pump coronary revascularization in patients with low ejection fraction: a report from the society of thoracic surgeons national database. *Ann Thorac Surg* 2013;96(1):83-8.
5. Batuhan Ozay, Murat Sargin, Gunseli Abay, et al. The severity of positional mitral regurgitation during off-pump coronary artery bypass grafting. *The Heart Surg Forum* 2008;11(3):E145-51.
6. Ritam Chowdhury, Darcy White, Patrick Kilgo, et al. Risk factors for conversion to cardiopulmonary bypass during off-pump coronary artery bypass surgery. *Ann Thorac Surg* 2012;93(6):1936-41.
7. Jean-Francois Legare, Karen J. Buth, Gregory M. Hirsch. Conversion to on pump from OPCAB is associated with increased mortality: results from a randomized controlled trial. *Eur J of Cardiothorac Surg* 2005;27(2):296-301.
8. Zhongmin Li, Ezra A. Amsterdam, Beate Danielsen, et al. Intraoperative

- conversion from off-pump to on-pump coronary artery bypass Is associated with increased 30-day hospital readmission. *Ann Thorac Surg* 2014;98(1):16-22.
9. James R. Edgerton, Todd M. Dewey, Mitchell J. Magee, et al. Conversion in off-Pump coronary artery bypass grafting: an analysis of predictors and outcomes. *Ann Thorac Surg* 2003;76(4):1138-43.
 10. Toshimasa Akazawa, Hirotaka Iizuka, Miyuki Aizawa, et al. The degree of newly emerging mitral regurgitation during off-pump coronary artery bypass is predicted by preoperative left ventricular function. *J Anesth* 2008;22(1):13-20.
 11. Takeshi Omae, Yasuyuki Kakihana, Akira Mastunaga, et al. Hemodynamic changes during off-pump coronary artery bypass anastomosis in patients with coexisting mitral regurgitation: improvement with milrinone. *Anesth Analg* 2005;101(1):2-8.
 12. Shane J. George, Sharif Al-Ruzzeh, Mohamed Amrani. Mitral annulus distortion during beating heart surgery: a potential cause for hemodynamic disturbance – a three-dimensional echocardiography reconstruction study. *Ann Thorac Surg* 2002;73(5):1424-30.
 13. Shugo Koga, Yukio Okazaki, Hiromi Kataoka, et al. Configurations of the mitral valve during off-pump coronary artery bypass grafting: endoscopic and three-dimensional analysis. *J Heart Valve Dis.* 2007;16(6):602-607.
 14. Hiroki Wakamatsu, Toshiki Watanabe, Yoshiyuki Sato, et al. Selective beta-1 receptor blockade further reduces the mechanically stabilized target coronary artery motion during beating heart surgery. *Innovations* 2010;5(5):349-354.

15. Ken Saito, Hiroyuki Okura, Nozomi Watanabe, et al. Influence of chronic tethering of the mitral valve on mitral leaflet size and coaptation in functional mitral regurgitation. *J Am Coll Cardiol Img* 2012;5(4):337-45.
16. Ryotaro Yamada, Nozomi Watanabe, Teruyoshi Kume, et al. Quantitative measurement of mitral valve coaptation in functional mitral regurgitation: In vivo experimental study by real-time three-dimensional echocardiography. *J Cardiol* 2009;53(1):94-101.
17. Liam Ryan, Benjamin Jackson, Landi Parish, et al. Quantification and localization of mitral valve tenting in ischemic mitral regurgitation using real-time three-dimensional echocardiography. *Eur J Cardiothorac Surg* 2007;31(5):839-4.
18. Yutaka Otsuji, Mark D. Handschumacher, Ehud Schwammenthal, et al. Insights from three-dimensional echocardiography into the mechanism of functional mitral regurgitation: direct in vivo demonstration of altered leaflet tethering geometry. *Circulation* 1997;96(6):1999-2008.
19. Toshiro Kumanohoso, Yutaka Otsuji, Shiro Yoshifuku, et al. Mechanism of higher incidence of ischemic mitral regurgitation in patients with inferior myocardial infarction: quantitative analysis of left ventricular and mitral valve geometry in 103 patients with prior myocardial infarction. *J Thorac Cardiovasc Surg* 2003;125(1):135-43.
20. Henrik Jensen, Morten O. Jensen, Morten H. Smerup, et al. Three-dimensional assessment of papillary muscle displacement in a porcine model of ischemic mitral regurgitation. *J Thorac Cardiovasc Surg* 2010;140(6):1312-8.

21. Yutaka Otsuji, Robert A, Levine, Masaaki Takeuchi, et al. Mechanism of ischemic mitral regurgitation. *Journal of Cardiology* 2008;51(3):145-56.

Table 1 Hemodynamic parameters in each position

	Control position	LAD position	RCA position	LCX position	<i>P</i> value by ANOVA
Heart rate (bpm)	94.2±7.5	89.1±10.0	90.1±8.2	88.8±11.5	0.35
Systolic blood pressure (mmHg)	69.9±7.7	57.2±8.2 ⁺	54.1±7.4 ⁺	48.9±7.1 ⁺	<0.001
Diastolic blood pressure (mmHg)	38.1±5.1	31.2±5.7 ⁺⁺	32.0±4.1 ⁺⁺	30.7±5.5 ⁺	<0.001
Mean blood pressure (mmHg)	49.8±5.9	42.7±8.0	40.4±5.1 ⁺	37.8±6.4 ⁺	<0.001
Systolic pulmonary artery pressure (mmHg)	20.2±1.7	19.4±2.8	18.9±1.8	18.4±3.1	0.12
Diastolic pulmonary artery pressure (mmHg)	8.3±2.0	8.4±2.9	8.3±2.2	7.7±2.6	0.46
Mean pulmonary artery pressure (mmHg)	16.4±3.0	16.6±2.5	16.6±2.5	15.2±4.1	0.48
Central venous pressure (mmHg)	8.0±0.9	8.2±1.2	8.8±1.2 ⁺	9.4±1.9 ⁺⁺	0.001
Cardiac output (L/min)	3.6±0.8	3.4±0.6	3.6±0.5	3.4±0.5	0.55

+ : P<0.01 vs control by Bonferroni

++ : P<0.05 vs control by Bonferroni

Table 2 Three-dimensional configuration of mitral valve complex

	Control position	LAD position	RCA position	LCX position	<i>P</i> value by ANOVA
AP diameter (mm)	27.17±2.13	26.66±2.00	27.02±1.67	26.79±2.01	0.93
ML diameter (mm)	30.95±1.49	31.00±2.17	30.34±1.60	31.42±1.86	0.37
Annular circumference (mm)	94.72±5.96	94.85±6.77	94.29±3.44	96.43±5.19	0.73
Annular area (cm ²)	6.87±0.81	6.85±0.90	6.81±0.51	7.07±0.76	0.81
Annular height (mm)	4.41±1.82	5.40±1.71	4.74±1.14	5.37±1.53	0.14
Maximum tenting length (mm)	2.93±1.33	2.71±0.95	3.68±0.95	4.10±0.94	0.003
Mean tenting length (mm)	0.65±1.01	0.46±0.84	1.31±0.60	1.54±0.63	0.001
Tenting Volume (cm ³)	0.70±0.30	0.65±0.27	0.79±0.23	0.95±0.34	0.02
Tethering distance (APM) (mm)	29.80±3.68	28.78±1.61	28.87±4.04	28.98±2.94	0.81
Tethering distance (PPM) (mm)	32.92±4.37	33.67±4.63	32.76±3.75	33.20±3.48	0.89
Angle α1 (degree)	58.58±11.62	51.98±7.20	54.27±8.12	53.00±8.09	0.33
Angle α2 (degree)	50.70±8.25	49.93±10.49	50.92±9.84	44.48±8.58	0.18

AP diameter: anterior-posterior diameter, ML diameter: medial-lateral diameter

APM: anterior papillary muscle, PPM: posterior papillary muscle

Table 3 Three-dimensional coordinates of papillary muscles

		Control	LAD position	RCA position	LCX position	<i>P</i> value by ANOVA
APM	x (mm)	20.4±9.9	12.9±6.5	17.9±6.0	17.5±4.5	0.22
	y (mm)	25.3±4.7	25.6±4.1	25.2±6.3	25.3±4.0	0.99
	z (mm)	3.0±3.5	2.8±3.9	3.9±4.5	-0.1±7.3	0.38
PPM	x (mm)	7.2±9.7	7.5±7.4	10.0±9.6	7.0±9.1	0.82
	y (mm)	29.6±3.1	32.2±5.8	27.6±11.8	31.4±3.3	0.6
	z (mm)	-2.9±4.8	-9.6±3.6	-3.9±3.2	-9.3±3.6	0.004

APM: anterior papillary muscle, PPM: posterior papillary muscle

Figure Legends

Figure 1. A schematic overview of animal preparation.

A swine was placed in a supine position. Electrocardiogram, respirator, venous injection line, femoral arterial line and Swan-Ganz catether were introduced.

Figure 2. The form of the displacement of the heart.

The beating heart was positioned in four positions in order by control position, LAD position, RCA position and LCX position.

Figure 3. Study Protocol.

The echocardiographic and hemodynamic data was acquired in each position.

Figure 4. Parameters for assessment of mitral valve.

The three-dimensional geometric changes of the mitral valve were assessed by REALVIEW[®] software. Annular parameters (AP diameter, ML diameter, annular circumference and annular height) and tenting parameters (maximum tenting length, mean tenting length and tenting volume) were measured. Maximum tenting length was defined as the length between the most tenting point of the mitral leaflet and the annular plane. Tenting volume was defined as the cubic content surrounded by the leaflet and the annular plane.

Figure 5. Papillary muscles' position by three-dimensional echocardiography.

a) Three-dimensional coordinates of the midpoint of the anterior mitral annulus,

the contralateral point of A on the aortic annulus (B), the midpoint of the posterior mitral annulus (C), the tip of the anterior papillary muscle (APM) and the tip of the posterior papillary muscles (PPM).

b) Tethering distance and angle α are shown by schema.

Figure 6. Three-dimensional configuration of mitral valve by REALVIEW[®]

The tenting of mitral leaflets was increased in the dislocated positions, especially in LCX position.

Figure 7. The correlation between tenting volume and angle α_2 .

- a) Angle α_2 showed the statistically significant correlation with the tenting volume.
- b) This graph revealed the relation between the control position and the LCX position in each case. Tenting volume tended to increase and angle α_2 tended to decrease by the displacement of the heart in many cases.

Figure 8. The schema of the displacement of the papillary muscles in each heart position (short axis view via apex). Three-dimensional coordinates of papillary muscles were shown as (x mm, y mm, z mm).

The tip of the PPM and the APM dislocated to the medial side with narrowing of left ventricle in LCX position.

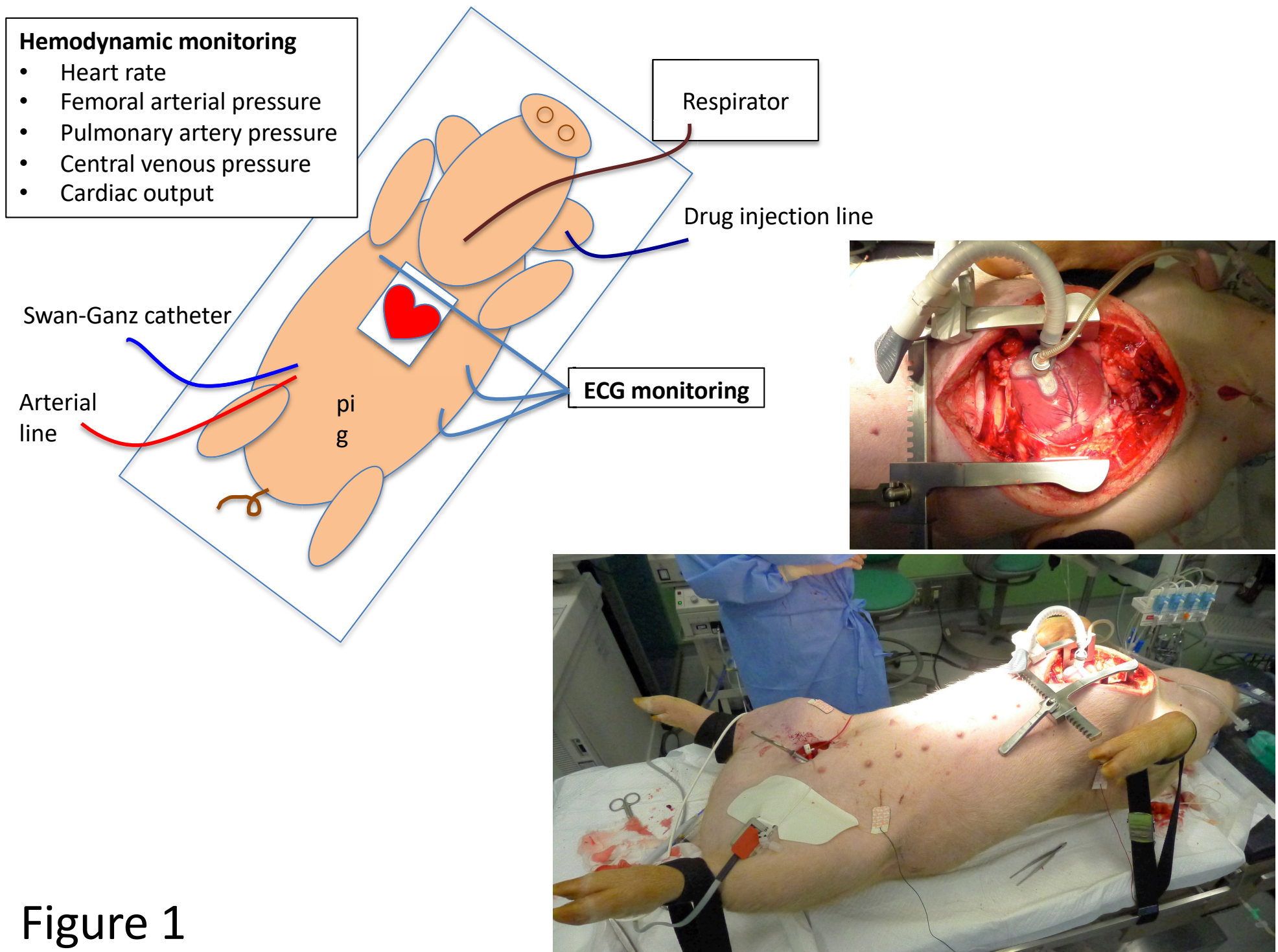


Figure 1

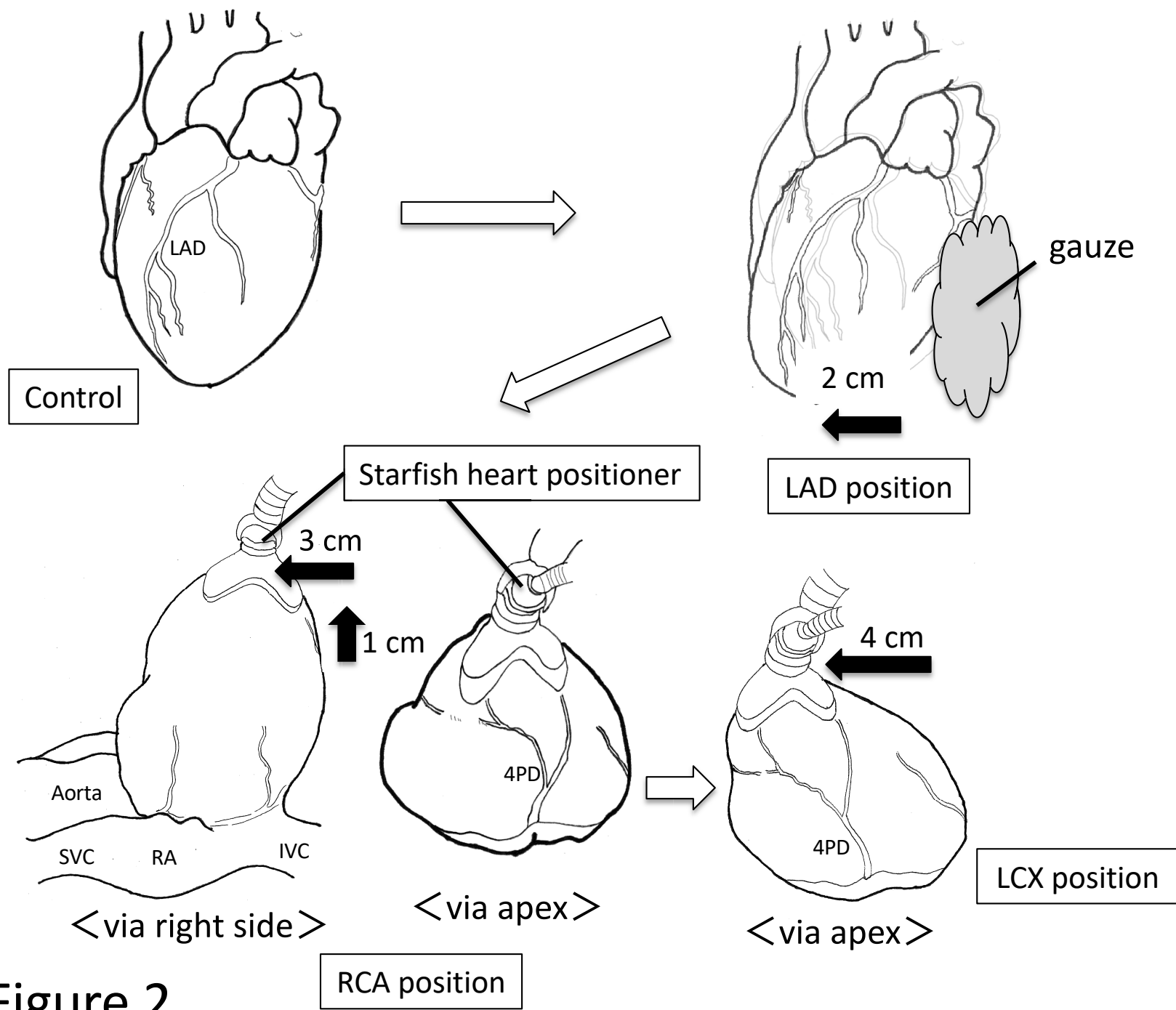


Figure 2

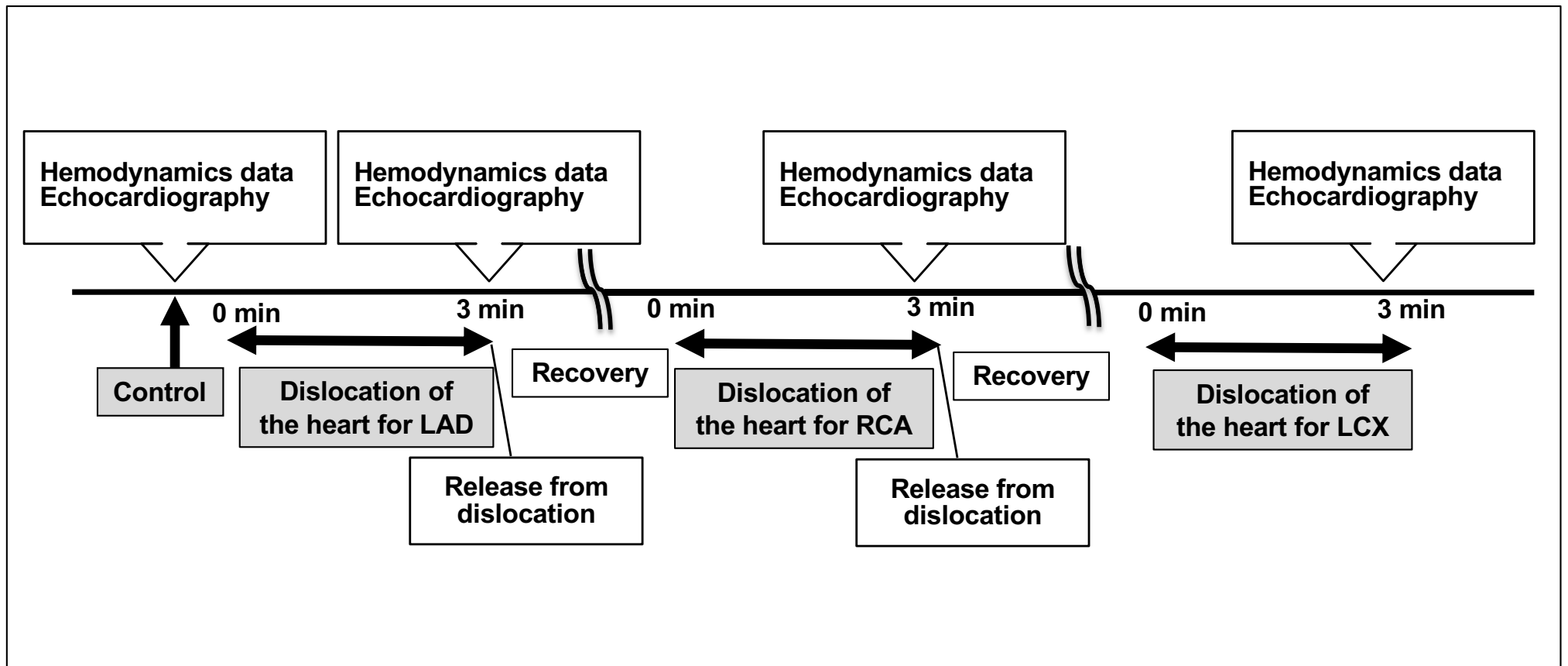
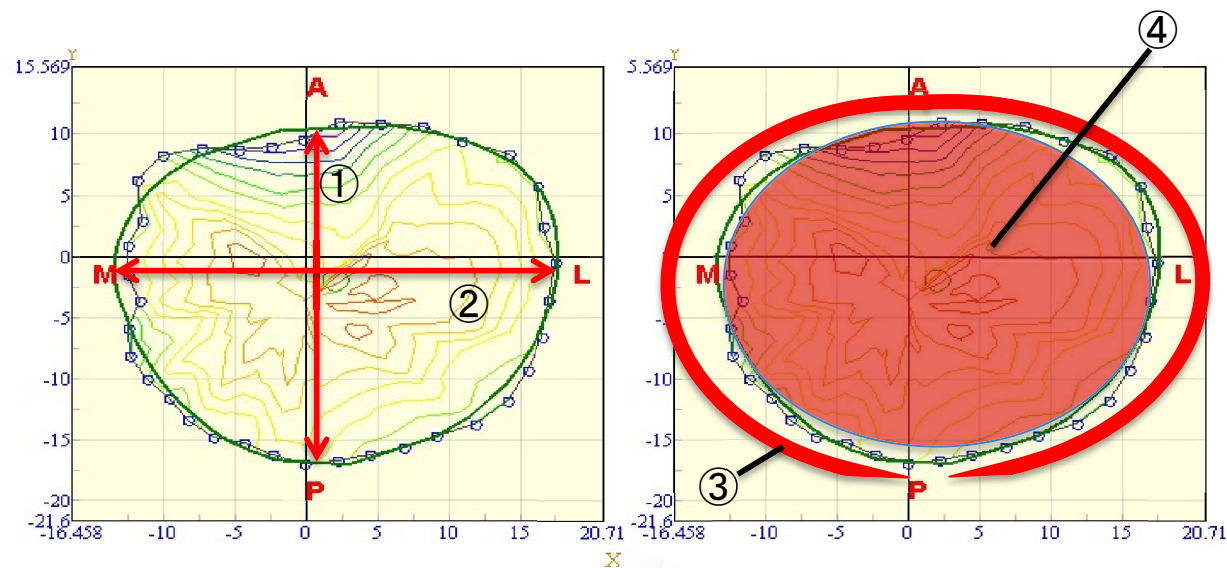


Figure 3



- ① AP diameter
- ② ML diameter
- ③ Annular circumference
- ④ Annular area
- ⑤ Annular height
- ⑥ Maximum tenting length
- ⑦ Mean tenting length
- ⑧ Tenting volume

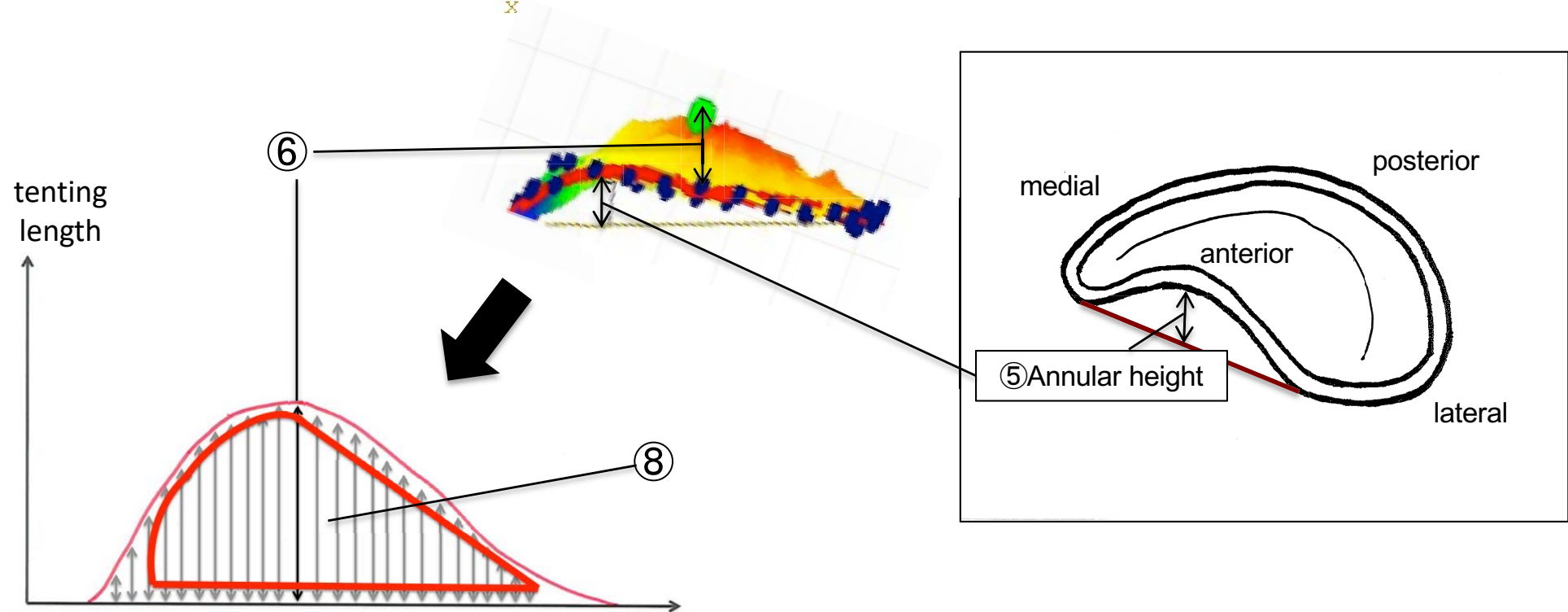


Figure 4

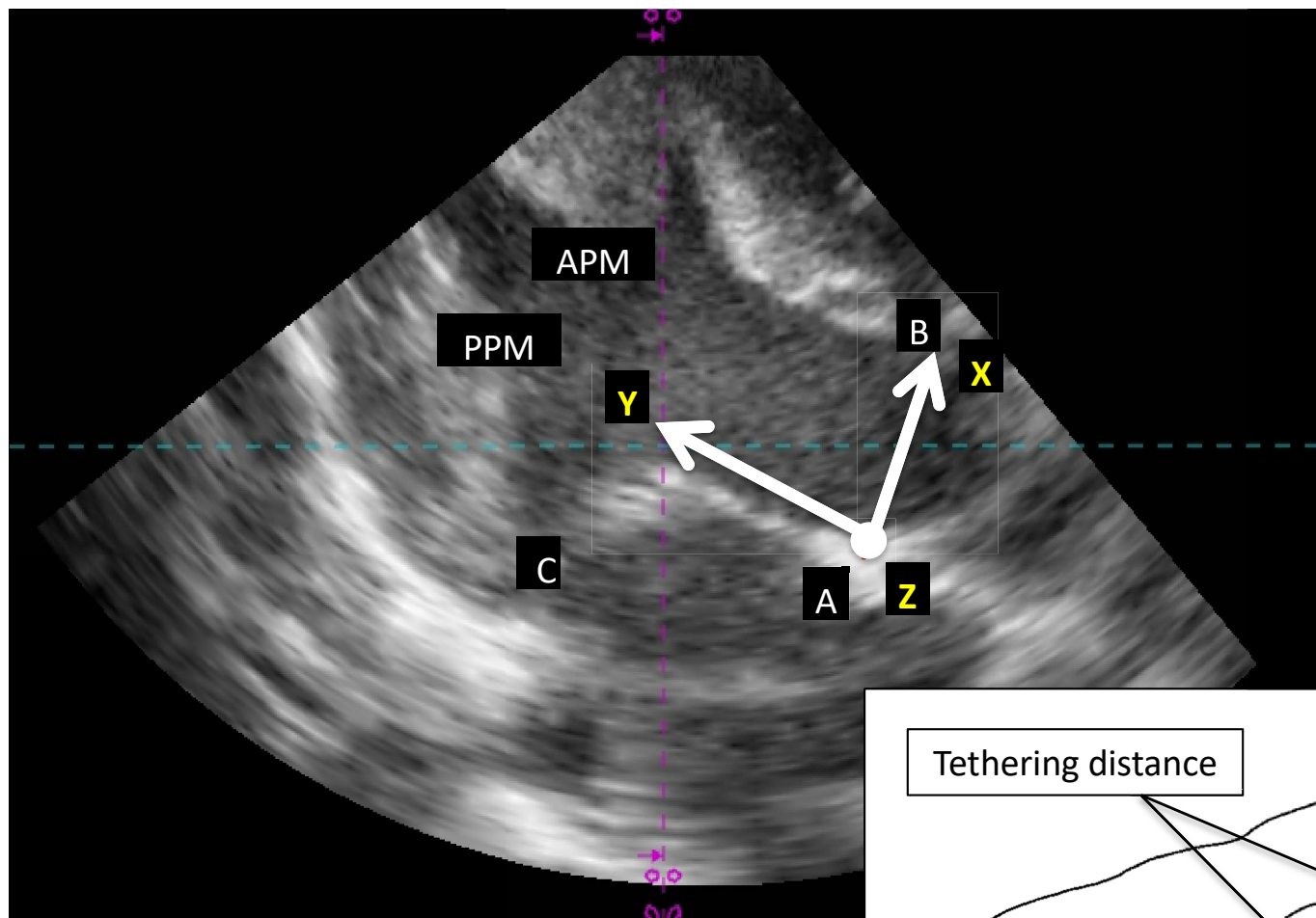


Figure 5a

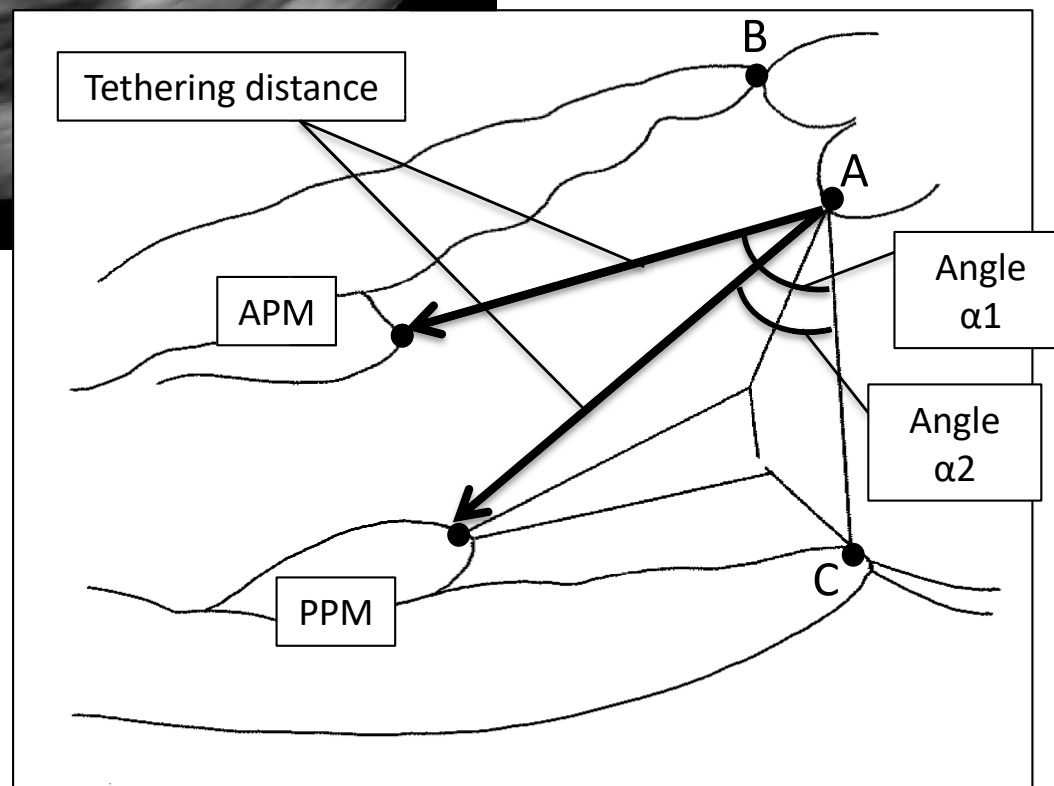
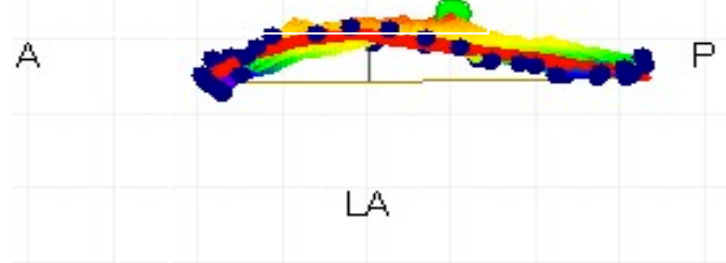
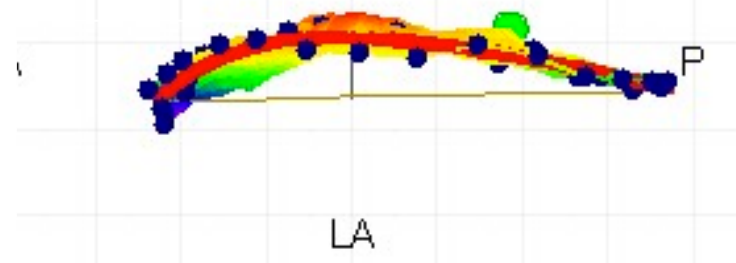


Figure 5b

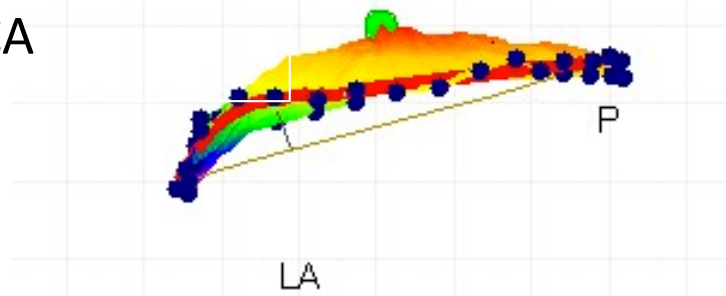
Control



LAD



RCA



LCX

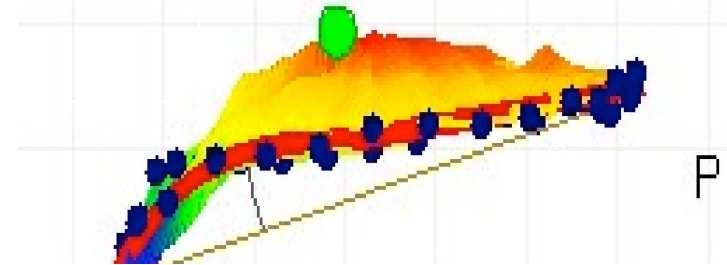


Figure 6

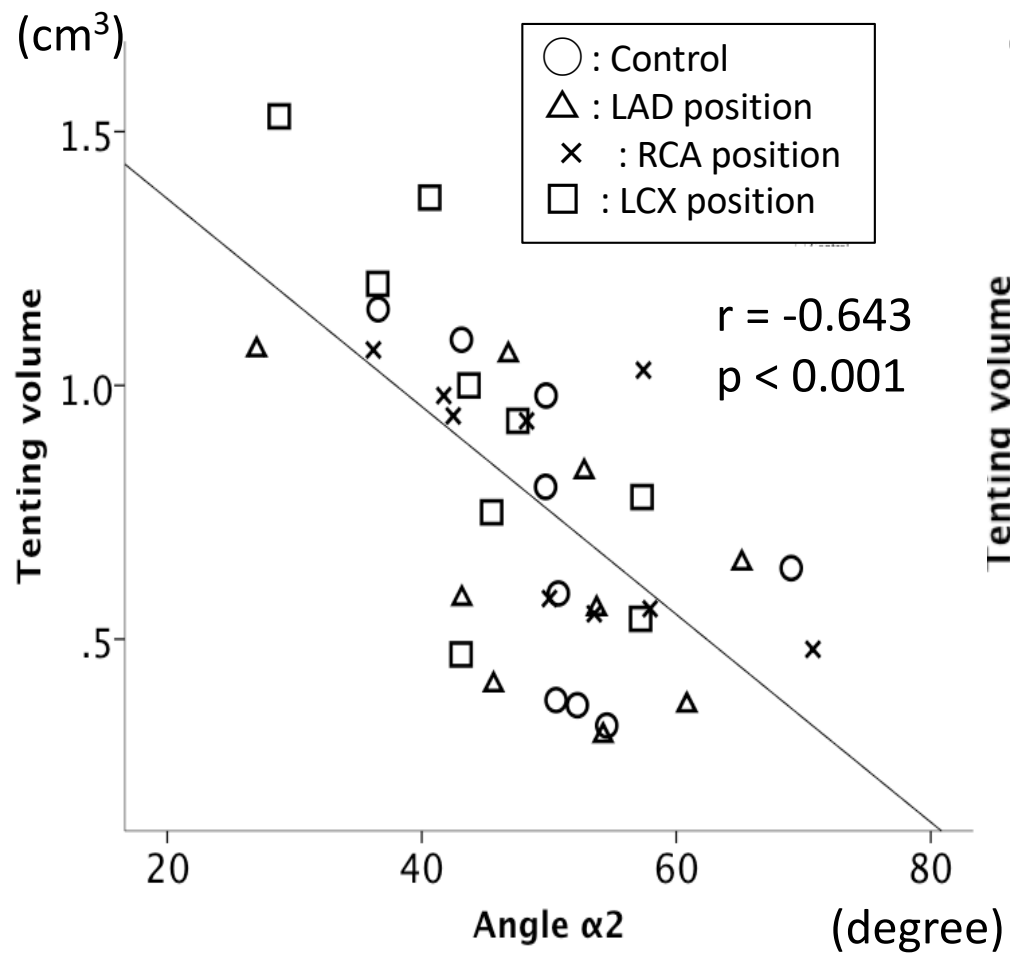


Figure 7a

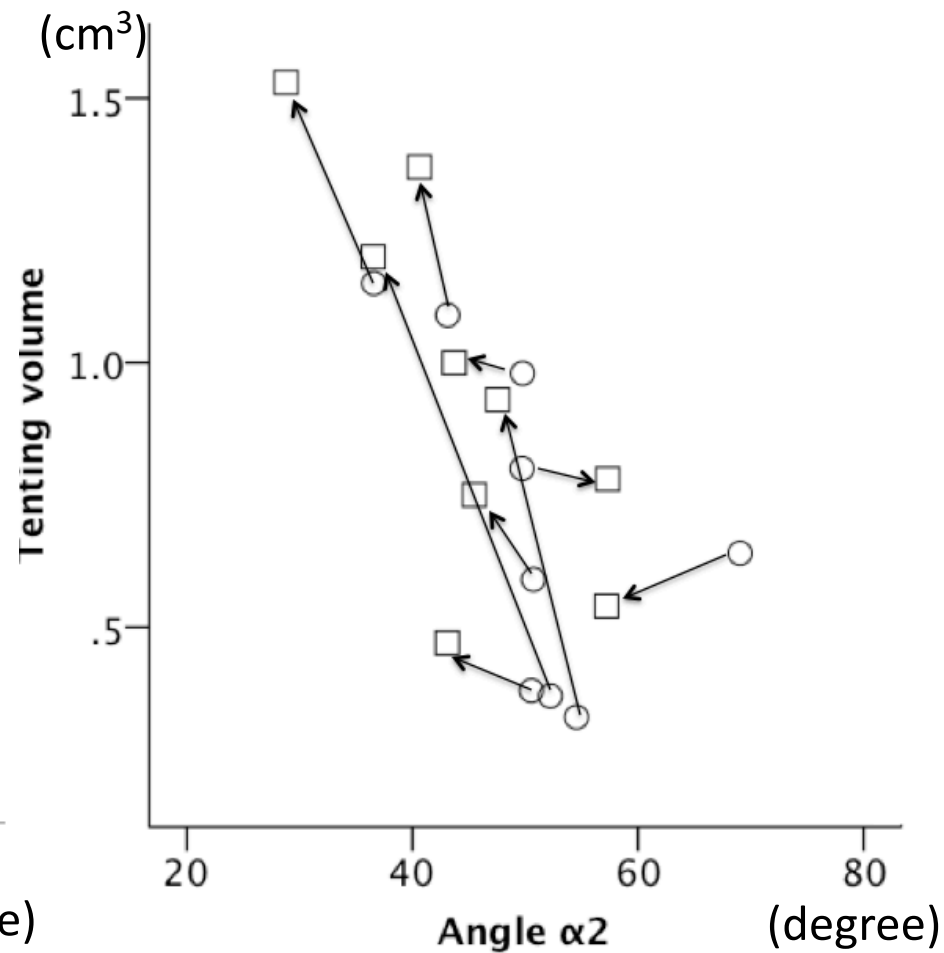


Figure 7b

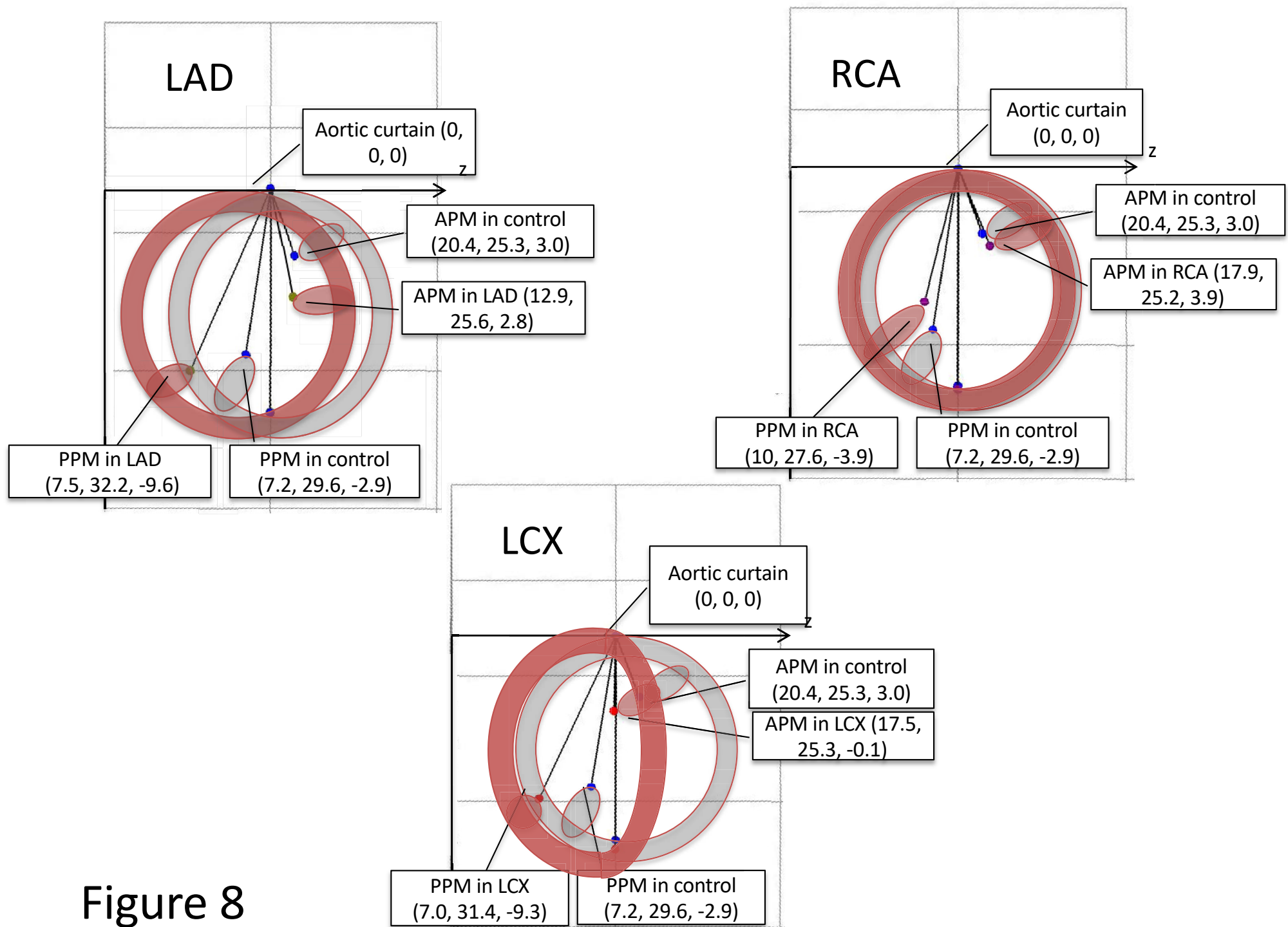


Figure 8